Surface Tension Measurement of Polystyrene Melts in Supercritical Carbon Dioxide

H. Park,[†] C. B. Park,[‡] C. Tzoganakis,[†] K. H. Tan,[§] and P. Chen*,[†]

Department of Chemical Engineering, University of Waterloo, 200 University Avenue, Waterloo, Ontario, Canada N2L 3G1, Microcellular Plastics Manufacturing Laboratory, Department of Mechanical and Industrial Engineering, University of Toronto, 5 King's College Road, Toronto, Ontario, Canada M5S 3G8, Epson R&D, 3145 Porter Drive, Suite 104, Palo Alto, California 94304-1224

This paper introduces an experimental method that uses Axisymmetric Drop Shape Analysis-Profile (ADSA-P) to measure the surface tension of polymer melts in supercritical carbon dioxide. The method is verified by experiments in air and nitrogen, where reproducibility tests and statistical analyses are performed. The surface tension of polystyrene (PS) melts in supercritical carbon dioxide is obtained, while the gas solubility is correlated with the surface tension value determined under various pressures. The Sanchez−Lacombe (S−L) equation of state (EOS) is applied to estimate the pressure−volume−temperature (PVT) data of the PS/supercritical-carbon-dioxide mixtures, which gives density data. The relationship between surface tension and density is described by the empirical Macleod equation. To characterize the stability of pendant drops formed by the polymer melt, the Bond number is determined to be useful; in particular, a stable pendant drop is obtained when the Bond number is in the range of 0.4−0.8.

Introduction

The primary objective of this work is to measure the surface tension of polystyrene (PS) melts in supercritical carbon dioxide. Surface tension provides valuable information about how to proceed with technological processes, such as foaming, particle (pigment) suspensions, wetting, and polymer blending.[1] Among the methods commonly used to measure surface tension, drop shape methods are distinguished by the premise that the shape of a sessile or a pendant drop is governed by a combination of surface tension and gravity. In principle, when gravitation and surface tension effects are comparable, the shape of a drop or a bubble can be used to determine the surface tension. The drop shape methods have many advantages because of their simple, yet versatile, mechanics. For example, they require only small amounts of the liquid, as compared with other methods, such as the Wilhemy plate technique.[2] The drop shape methods also facilitate the study of both liquid−vapor and liquid−liquid interfacial tensions. Furthermore, these techniques can be applied to materials ranging from pure solvents to concentrated solutions, and from organic liquids to molten metals.[3] They are highly adaptable, considering the fact that conditions within the sample cell can range from low to high temperatures, and from vacuum to high pressures.

The pendant drop method, which is a common one for measuring the surface and interfacial tensions of a liquid, is a robust method that is independent of contact angle; it entails a simple experimental setup and has been used extensively for evaluating the surface tension of polymers, liquid crystals, and other low-molar-mass liquids.[4] This method involves the determination of a drop profile of one denser liquid suspended in another liquid at mechanical equilibrium of the interface. The balance between gravity and surface forces determines the drop profile. Recent progress in image analysis and data acquisition systems has made it possible to obtain direct digitalization of a drop image with the aid of a video frame grabber and a digital camera. The digital signals are further analyzed using different algorithms to determine the surface/interfacial tension from the drop profile.[5−9]

Despite the theoretical simplicity of using sessile and pendant drops for determining the surface tension of polymer melts, research in this area has been limited, because of the experimental difficulty in handling and ensuring the equilibrium of highly viscous melts.[10−20] The Axisymmetric Drop Shape Analysis (ADSA) approach relies on a numerical integration of the Laplace equation of capillarity. This numerical procedure unifies both the sessile drop and the pendant drop methods. Recently, ADSA has been used in application for determining polymer melt surface tensions at high temperature and high pressure.[21]

The objective of this research is to establish an ADSA-based approach for evaluating the surface tension of polystyrene melts in supercritical carbon dioxide. The dependence of surface tension on temperature and pressure is investigated, and the interplay between surface tension and solubility is studied.

Experimental Section

Materials. Polystyrene (PS, Styron 685D, M_n = 120 000, polydispersity index = 2.6) was kindly supplied by Dow Chemical Company. Carbon dioxide (99.99% purity, Supercritical Fluid Chromatographic grade, PRAXAIR) was used as a supercritical fluid in all of the experiments. Nitrogen (99.99% purity, PRAXAIR) was used as an inert gas for the purpose of measuring the surface tension of PS. No chemicals were modified prior to use.

Axisymmetric Drop Shape Analysis-Profile (ADSA-P). The pendant drop method involves the suspension of a drop of one liquid at the tip of a capillary in another fluid (either a gas or another liquid). The interfacial tension can be ascertained from

* To whom correspondence should be addressed. E-mail: p4chen@cape.uwaterloo.ca.

[†] Department of Chemical Engineering, University of Waterloo.

[‡] Microcellular Plastics Manufacturing Laboratory, Department of Mechanical and Industrial Engineering, University of Toronto.

[§] Epson R&D.

10.1021/ie0509084 CCC: $33.50
Published on Web 02/02/2006

Table 1. Characteristic Parameters for the Sanchez−Lacombe Equation of State (S−L EOS)

substance	characteristic pressure, P^* (MPa)	characteristic density, ρ^* (kg/m^3)	temperature, T (K)	reference
polystyrene, PS	387.0	1108	739	25
CO_2	720.3	1580	$208.9 + 0.459T - (7.56 \times 10^{-4})T^2$	25

Table 2. Binary Interaction Parameters of Two Different Temperatures[a]

parameter	Value at 210 °C	Value at 230 °C
K_{12}	−0.1977	−0.2343

[a] Data taken from ref 25.

an analysis of the drop profile, where the density difference between the two fluids is used as an input parameter. The classical Laplace equation of capillarity is the basis for all static analyses of interfacial and surface tensions. It states that the pressure difference across a curved interface can be described by

$$\frac{1}{R_1} + \frac{1}{R_2} = \frac{\Delta P}{\sigma} \tag{1}$$

where R_1 is the radius of curvature in the plane of paper, R_2 the radius of curvature in a plane perpendicular to paper, ΔP the pressure difference across the curved interface, and σ the interfacial tension.

In their theoretical research, Bashforth and Adams successfully transformed the Laplace equation into convenient dimensionless forms, and numerical solutions with an accuracy to 4−5 decimal places were tabulated.[22] In earlier experimental studies, the shape of liquid menisci was measured manually and interfacial tensions were interpreted with different sets of tables. Progress in image analysis and data acquisition has made it possible to obtain a direct digitalization of the drop image with the aid of a video frame grabber and digital camera. The technique of Axisymmetric Drop Shape Analysis-Profile (ADSA-P) has been developed to determine liquid−fluid interfacial tensions from the shape of axisymmetric menisci.[4] In this technique, drop images are digitized with subpixel resolution, and experimental drop profiles are compared with theoretical profiles governed by the Laplace equation of capillarity. A least-squares algorithm is used with the interfacial (surface) tension as one of the adjustable parameters. Other parameters, such as drop volume, surface area, and radius of curvature, can also be obtained. The ADSA-P method is used in this study; additional details are discussed in other publications.[5,9]

Density Determination. The mass densities of PS, PS saturated with carbon dioxide, and carbon dioxide were each determined using the Sanchez−Lacombe (S−L) equation of state (EOS),[23,24] as shown below:

$$\tilde{\rho}^2 + \tilde{P} + \tilde{T}\left[\ln(1-\tilde{\rho}) + \left(1 - \frac{1}{r}\right)\tilde{\rho}\right] = 0 \tag{2}$$

where $\tilde{\rho}$ is the reduced density, $\tilde{P}$ the reduced pressure; $\tilde{T}$ the reduced temperature, and r the number of sites occupied by a molecule, the latter of which is defined as

$$\tilde{P} = \frac{P}{P^*},\ \tilde{\rho} = \frac{\rho}{\rho^*},\ \tilde{T} = \frac{T}{T^*},\ r = \frac{MP^*}{RT^*\rho^*} \tag{3}$$

where ρ is the density, P the pressure, T the temperature, M the molecular weight, and R the gas constant. In this equation, the characteristic parameters—P^*, ρ^*, and T^*—of the S−L EOS for the mixture were evaluated using the following mixture rules:

$$P^* = \sum_i \sum_j \phi_i \phi_j P_{ij}^* \tag{4}$$

$$P_{ij}^* = (1 - k_{ij})(P_i^* P_j^*)^{0.5} \tag{5}$$

$$T^* = P^* \sum_i \frac{\phi_i^\circ T_i^*}{P_i^*} \tag{6}$$

$$\frac{1}{r} = \sum_i \frac{\phi_i^\circ}{r_i^\circ} \tag{7}$$

$$\phi_i^\circ = \frac{(\phi_i P_i^* T_i^*)}{\sum_j (\phi_j P_j^* T_j^*)} \tag{8}$$

$$\phi_i = \frac{(w_i/\rho_i^*)}{\sum_j (w_i/\rho_i^*)} \tag{9}$$

where T_i^*, P_i^*, ρ_i^*, and r_i° represent the characteristic parameters of the component i in its pure state. The characteristic parameters for calculating the density using the S−L EOS are given in Table 1. The binary interaction parameter (k_{12}) was determined, to minimize the relative experimental deviation at each given temperature.[25] The determined binary interaction parameters of two different temperatures are listed in Table 2.

Apparatus and Procedures. The ADSA-P was used to measure the surface tension of PS in supercritical carbon dioxide. A schematic of the pendant drop apparatus is shown in Figure 1. An IsoStation Vibration Isolated Workstation (labeled as "1" in Figure 1) was used to isolate the vibration-sensitive elements from the floor motion or vibration. To illuminate the pendant drop, a light source (labeled as "2" in Figure 1) was used. Generally, a frosted glass diffuser (labeled as "3" in Figure 1) was used between the light source and the pendant drop. The light diffuser provides a uniformly bright background, which results in images of high contrast. Pendant drops could be formed by attaching one polymer of higher density to a heated stainless steel holding rod (labeled as "4" in Figure 1). Alternatively, pendant drops could also be obtained by extruding a higher-density polymer with a heated stainless steel syringe (4). The use of a syringe holder allowed for the manual dispensation of polymer melt drops. A high-pressure optical viewing cell (labeled as "5" in Figure 1) was used to melt the polymer within the fluid, which had a lower density. The optical viewing cell was fixed on an XYZ stage (labeled as "6" in Figure 1) that could be manipulated to finely adjust the position of the drop in three directions. A microscope system, including a microscope (labeled as "7" in Figure 1) and CCD camera (labeled as "8" in Figure 1), was used to take drop images and export image signals to a monochromatic monitor (labeled as "9" in Figure 1) and a computer (labeled as "10" and "11" in Figure 1). The microscope and camera were then mounted on another *XYZ* stage (labeled as "12" in Figure 1).

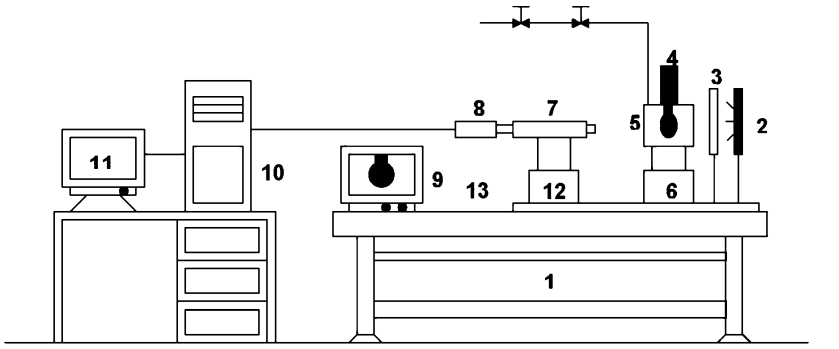

Figure 1. Schematic of the pendant drop apparatus.

The stage was also adjustable in three directions and could be deployed to alter the angle between the microscope and the horizon. The entire optical system was mounted and aligned on an optical rail (labeled as "13" in Figure 1).

The computer (10) has a high-accuracy, programmable frame grabber board for a PCI bus, which accepts video signals in many different monochrome formats and then digitizes the image. The board either stores the digitized data to the host computer's system memory or transfers the digitized data to the computer's display images in real time. An ADSA-P program was used to analyze images and implement a numerical procedure that yielded various results, including interfacial tensions, contact angles, and other parameters.

Most cameras and lenses produce slightly distorted images, and this distortion can cause major errors in the final results, particularly in the case of interfacial tension. A square reticule was used to check the distortion of the optical system. The ADSA-P can correct the drop image for optical distortion by invoking the knowledge of a calibration grid image and the spacing between the grid lines.[4]

The optical viewing cell, which was used to hold the pendant drop, had two sapphire windows mounted perpendicular to the cell axis (see Figure 2). Measurements of surface or interfacial tensions involving low-molecular-weight liquids under atmospheric pressure indicated that the distortion of the sapphire window was insignificant. It is believed that the distortion incurred by the sapphire window under a pressure of <30 MPa was similarly negligible. Therefore, most of the distortion caused by the sapphire window was insignificant.

The optical viewing cell consists of an electrically heated, stainless steel hollow cylinder chamber in which the pendant drop was formed. The inside of the cell is cylindrical in shape, with dimensions of 30 mm (diameter) by 25 mm (length). Two flat optical-quality sapphire windows (Meller Optics, Inc.), sandwiched between brass and Teflon gaskets within the chamber, permit illumination and viewing of the drop. The temperature of the cell was maintained with an accuracy of ± 1 °F (0.5 °C) using a temperature controller (Fuzypro F16) in conjunction with a type-K thermocouple. The thermocouple was located $\sim$30 mm from the pendant drop, and the temperature reading was taken as the temperature for the entire pendant drop environment. Several threaded ports were drilled into the cell to allow for the placement and easy removal of the sapphire window for cleaning purposes. The syringe was used to produce pendant drops through the capillary. A pressure tube was attached to feed the gas into the cell by Swagelok male connections with tapered pipe threads (i.e., NPT).

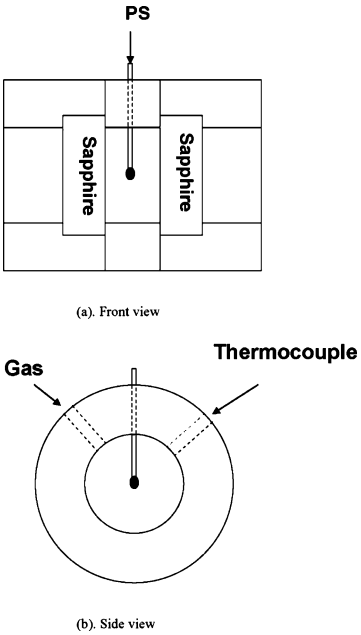

Figure 2. Schematic of the optical view cell: (a) front view and (b) side view.

A PS pellet and the holding rod were both cleaned with ethanol. The holding rod and the optical viewing cell were heated to the desired temperature. A polymer pellet was placed in a position to ensure contact between it and the bottom surface of the rod. The pendant was created upon melting the PS pellet and held at the bottom surface of the rod (of 1.5 mm in diameter). Image acquisition of the pendant drop profile was performed and digitalized each minute. When the observed surface tension variation was small enough ($<5\%$), for at least 1 h, the surface was considered to have reached equilibrium and the surface tension was adopted as an equilibrium surface tension and used for further analyses.

Results and Discussion

Method Verification. The surface tension of water and acetone at room temperature and atmospheric pressure was measured to validate the apparatus. Table 3 demonstrates that the measurement data collected are consistent with the data found in other studies.[26] The surface tension of water was

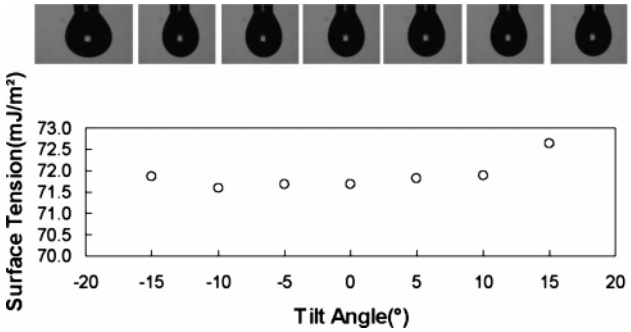

Figure 3. Effect of tilt angle on surface tension of water; the tile angle is defined as the angle between the symmetric line of the drop and a vertical line.

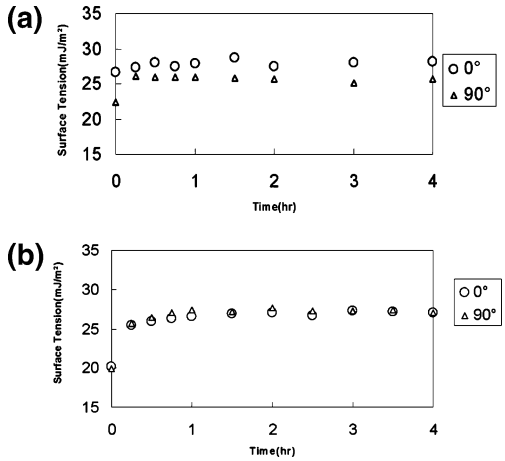

Figure 4. Effect of axis symmetry on the surface tension of polymers melts: (a) non-axisymmetric drop and (b) axisymmetric drop. The angles of 0° and 90° represent the respective direction of the microscope from the drop.

Table 3. Comparison of Measured Surface Tension with Literature Values

		Surface Tension (mJ/m^2)	
substance	density	this work (at 24.5 °C)	literature value[26]
water	0.998	72.10 ± 0.032	72.14 (at 25 °C)
acetone	0.7899	23.52 ± 0.008	23.70 (at 20 °C)

measured at different tilt angles; the results are shown in Figure 3. When the pendant drop was tilted, the surface tension values changed slightly with the angle variation.

The symmetry about the axis is one of the critical assumptions in ADSA-P. This assumption is valid for most Newtonian fluids; however, it is not easy to obtain an axisymmetric polymer drop, because of the initial configuration of the polymer sample and high polymer melt viscosity. This symmetry was examined from an experimental perspective, to measure the surface tension of the polymers. The image of the sample drops was grabbed and analyzed using ADSA-P in two different directions, which were perpendicular to each other. If the axis symmetry is not secured, the surface tension may have an error of 5% (see Figure 4). After the axis symmetry is secured, the margin of error can be decreased to ~1%. By measuring the volume of the drop, the axis symmetry was thus reconfirmed: The density was calculated by assuming that no reaction occurs at high temperatures. The density deviation can be decreased from 5% to 1%, using an axisymmetric drop, as is evident in Figure 5.

The reproducibility of the experiment was tested by measuring the surface tension of the PS melts in N_2 at different temperatures. Figure 6 illustrates the surface tension as a function of the following temperatures: 210, 200, 190, and 180 °C. For

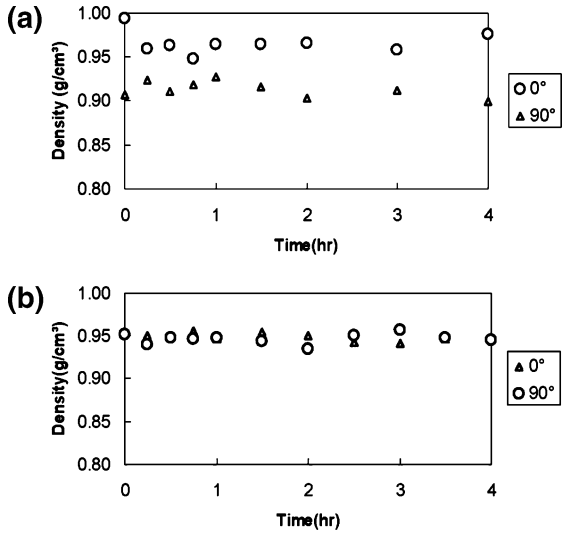

Figure 5. Effect of axis symmetry on the density of polymer melts: (a) non-axisymmetric drop and (b) axisymmetric drop. The angles of 0° and 90° represent the respective direction of the microscope from the drop.

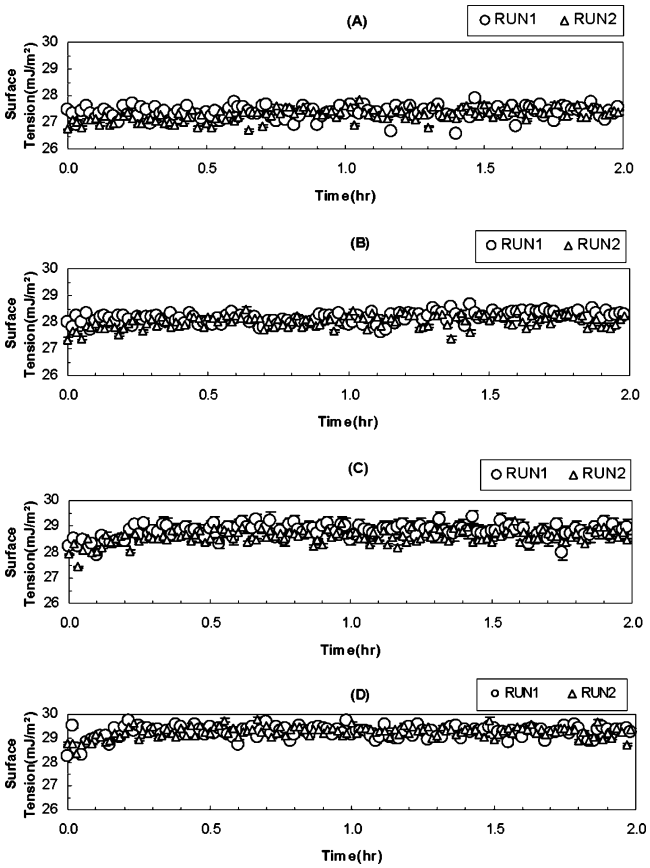

Figure 6. Reproducibility test: results of two runs for the surface tnesion of polystyrene (PS) melts in N_2, as a function of temperature: (a) 210 °C, (b) 200 °C, (c) 190 °C, and (d) 180 °C. The error bars are the 95% confidence limits are calculated from ADSA-P for each image.

each temperature, two runs were conducted. The surface tension measurements exhibited good consistency from run to run. The polymer surface tension in N_2 was further measured in the order of decreasing temperature. This is illustrated in Figure 7 at four different temperatures: 210, 200, 190, and 180 °C. The surface tension values from this experiment proved to be consistent with the data from two other studies.[12,16] The question of whether the surface tension values of two consecutive temperatures in Figure 7 are actually the same or significantly different can be

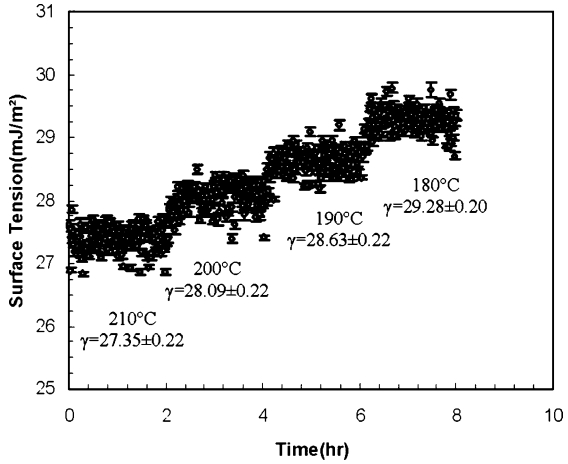

Figure 7. Surface tension of polystyrene for different temperatures in atmospheric pressure of N_2. The error bars are the 95% confidence limits calculated from ADSA-P for each image.

answered as follows. A *t*-distribution test was performed to ascertain the statistical difference of two consecutive surface tension values.[27] If the calculated *t*-value was higher than the critical tabulated value, this would suggest that the means are different at the selected significance level. If not, the values would then demonstrate no significant difference. Table 4 shows the surface tension values of 10 runs at different temperatures. In this study, the tabulated *t*-values were chosen to achieve a 95% confidence level in a two-sided question (*t*-critical (95%, 2s)).[27] The *t*-values were calculated to be able to compare the surface tensions of two temperatures. Table 5 indicates that the calculated *t*-values were higher than the tabulated values. This suggests that the surface tension values between two consecutive temperatures have significant differences at the 95% confidence level.

ADSA-P was also used to measure the density of polymer melts from the mass and the volume of a polymer drop; the mass could be preweighed and the volume was an output of the ADSA-P program. For the determination of density, it was assumed that the mass of the polymer drop was maintained constant during the experiment. Table 6 shows the density of PS melts at various temperatures. The *t*-distribution test was conducted using a method similar to that previously described.

Table 4. Surface Tension of PS Melts at Different Temperatures with Axisymmetric Drop Shape Analysis-Profile (ADSA-P)

run number	At 180 °C		At 190 °C		At 200 °C		At 210 °C	
	σ (mJ/m^2)	95% CL[a]	σ (mJ/m^2)	95% CL[a]	σ (mJ/m^2)	95% CL[a]	σ (mJ/m^2)	95% CL[a]
1	29.46	0.31	29.40	0.34	28.79	0.20	28.13	0.28
2	29.37	0.44	28.16	0.30	27.83	0.28	26.77	0.35
3	29.20	0.17	28.73	0.14	28.17	0.18	27.37	0.22
4	29.18	0.17	28.64	0.11	27.95	0.15	27.21	0.15
5	29.32	0.21	28.61	0.25	28.06	0.26	27.36	0.26
6	28.97	0.21	28.47	0.14	27.86	0.21	27.05	0.16
7	29.91	0.34	29.33	0.39	28.31	0.46	27.16	0.50
8	29.28	0.20	28.63	0.21	28.09	0.22	27.35	0.22
9	29.24	0.20	28.82	0.22	28.24	0.20	27.40	0.23
10	29.41	0.14	28.75	0.19	28.27	0.15	27.20	0.17
mean	29.33	0.25	28.75	0.37	28.16	0.28	27.30	0.35

[a] CL = confidence level.

Table 5. Statistical Comparison of Surface Tension Means at Various Temperatures

comparison	number of degrees of freedom, *n*	calculated *t* value, t_{cal}	t value of sides tabulated at a 95% confidence level, $t_{critical}$(95%,2s)	significant difference
σ(180 °C)/σ(190 °C)	9	4.134	2.262	yes
σ(190 °C)/σ(200 °C)	9	4.076	2.262	yes
σ(200 °C)/σ(210 °C)	9	6.092	2.262	yes

Table 6. Density of Polystyrene (PS) Melts at Different Temperatures Using ADSA-P

run number	At 180°C		At 190°C		At 200°C		At 210°C	
	ρ (g/cm^3)	95% CL	ρ (g/cm^3)	95% CL	ρ (g/cm^3)	95% CL	ρ (g/cm^3)	95% CL
1	0.97818	0.00385	0.97230	0.00404	0.96794	0.00270	0.96386	0.00330
2	0.97878	0.00460	0.97230	0.00404	0.96197	0.00385	0.96124	0.00431
3	0.98378	0.00189	0.97218	0.00217	0.96279	0.00247	0.95896	0.00270
4	0.97801	0.00383	0.97268	0.00292	0.96381	0.00353	0.95563	0.00350
5	1.01475	0.00274	1.00816	0.00363	1.01475	0.00377	1.00816	0.00395
6	1.01896	0.00343	1.00148	0.00311	1.01896	0.00501	1.00148	0.00403
7	0.95614	0.00220	0.90880	0.00324	0.95614	0.00474	0.90880	0.00463
8	0.98582	0.00298	0.98763	0.00326	0.96643	0.00338	0.95814	0.00404
9	1.00185	0.00320	0.97994	0.00294	0.97774	0.00279	0.96599	0.00411
10	0.97831	0.00238	0.97516	0.00334	0.96178	0.00320	0.97092	0.00314
mean	0.98746	0.01908	0.97506	0.02666	0.97523	0.02265	0.96532	0.02703

[a] CL = confidence level.

Table 7. Statistical Comparison of Surface Tension Means at Various Temperatures

comparison	number of degrees of freedom, *n*	calculated *t* value, t_{cal}	t value of sides tabulated at a 95% confidence level, $t_{critical}$(95%,2s)	significant difference
ρ(180 °C)/ρ(190 °C)	9	1.196	2.262	no
ρ(190 °C)/ρ(200 °C)	9	0.015	2.262	no
ρ(200 °C)/ρ(210 °C)	9	0.889	2.262	no

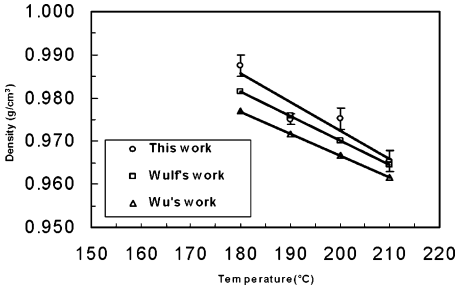

Figure 8. Comparison of this result and literature results of density for polystyrene in atmospheric pressure of N_2. The error bars are the 95% confidence level for ten experiments each.

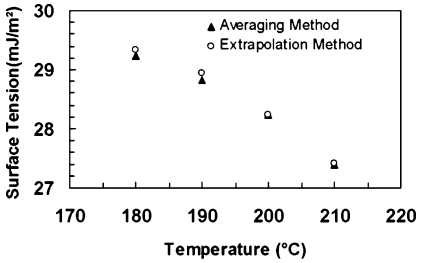

Figure 9. Surface tension obtained by the averaging method and extrapolation method at various temperatures.

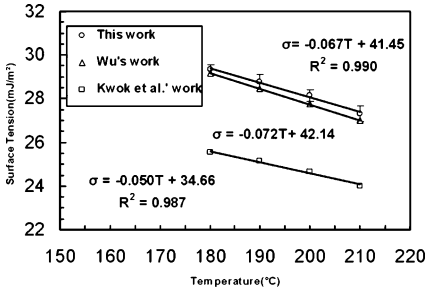

Figure 10. Comparison of this result and literature results of surface tension of PS in atmospheric pressure of N_2; the error bars are the 95% confidence level for 10 experiments each.

However, as shown in Table 7, the density values exhibit no significant difference from temperature to temperature. The errors involved in density calculations exceed the minute change in density with increasing temperature. The errors may be attributed to the way the drop volume is calculated with the ADSA-P program. In density calculations, two cut-off points have to be chosen manually near the boundary between the polymer and the metal holder; variations in the cut-off locations can cause the errors in volume calculations and, hence, the density results. Although the individual density measurements involve the errors, the overall decreasing trend with temperature is comparable with those of others (Figure 8). Note that the same variations in the cut-off locations may induce uncertainties in surface tension measurement; however, the surface tension change with temperature is sufficiently large, i.e., statistically significant. In this paper, only surface tension measurements were used to characterize the surface properties of the polymer melts.

Figure 9 shows two different methods for evaluating the equilibrium surface tension of PS melts as a function of temperature. In the extrapolation method, the extrapolation to zero (i.e., $t = \infty$) was taken from the graph of the surface tension versus $1/t^{1/2}$.[28,29] In the averaging method wherein the final data points were used, the average of the surface tension values was taken as the equilibrium surface tension when the change in surface tension was <0.0001 mJ m^{-2} s^{-1} for 1 h. The two types

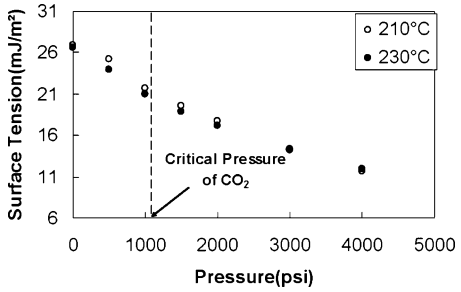

Figure 11. Pressure effect on the surface tension of PS in supercritical CO_2.

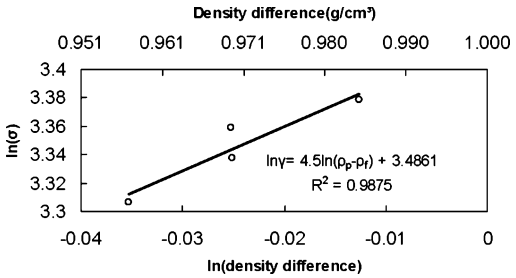

Figure 12. Relationship between surface tension and density for PS in atmospheric pressure in N_2. The density difference is defined the difference of density between the polymer and the gas.

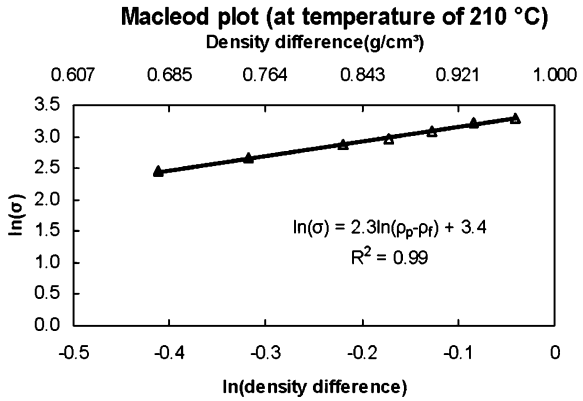

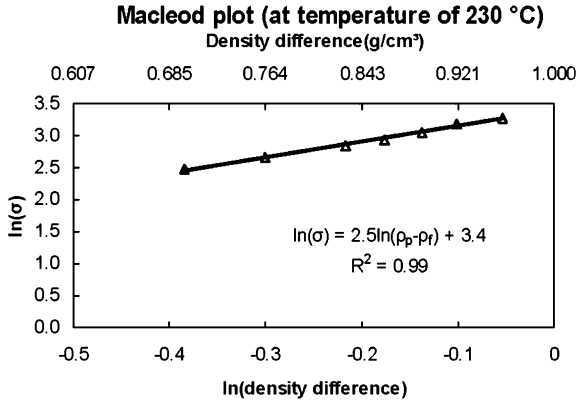

Figure 13. Relationship between surface tension and density for PS in supercritical CO_2. The density difference is defined the difference of density between the polymer and the gas.

of surface tension agreed well. This agreement indicates that both methods are valid for obtaining the equilibrium value. In this study, however, the "averaging method" was adopted for simplicity.

Figure 10 compares the surface tension values of PS in the nitrogen atmosphere obtained in this study with the data found

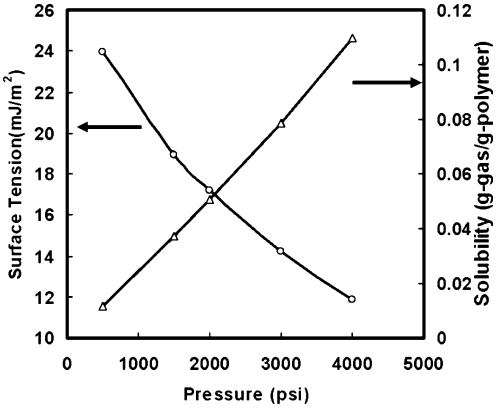

Figure 14. Relationship between the surface tension and solubility, as a function of pressure, for PS in supercritical CO_2 at a temperature of 230 °C.

in the literature. We have discovered that the results yielded by this study agree well with those of two other previous experiments.

Surface Tension of Polystyrene in Supercritical Carbon Dioxide. The surface tension of PS was measured in CO_2 under a wide range of pressures at two different temperatures (210 and 230 °C), and the results are shown in Figure 11. At higher pressures, the surface tension has a lower value. After the critical pressure (1071 psi) was reached, the surface tension continues to decrease.

The Relationship between Surface Tension and Density. The relationship between surface tension and density may be expressed by the generalized Macleod equation:[30]

$$\sigma = C(\rho_p - \rho_f)^n \tag{10}$$

where σ is the surface tension, C is a constant, ρ_p is the density of the polymer, ρ_f is the density of the fluid, and n is Macleod's exponent. The exponent n is close to 4 for many unassociated liquids of low-molecular-weight substances.[30,31] In this study, the Macleod's exponent is $n = 4.5$ at atmospheric pressure (see Figure 12), which is very similar to Wu's results.[12] At atmospheric pressure, the exponent has a higher value than that when a low-molecular-weight substance is used. This is because the polymer exhibits conformational restriction at the polymer surface. Figure 13 shows the relationship between surface tension and density difference for PS in supercritical CO_2. With an increased pressure in supercritical CO_2, the Macleod's exponent became $n \approx 2.5$ because the conformational restriction decreased. This correlation can be applied to predict the surface tension at various temperatures and pressures.

The Correlation between Surface Tension and Solubility. The surface tension and solubility as a function of pressure for PS in supercritical CO_2 at 230 °C are shown in Figure 14. As the pressure is increased, the solubility of CO_2 increases and the surface tension decreases.[21] This is reasonable when considering the fact that an increase in gas-phase pressure will likely induce more gas dissolution into the liquid phase. Surface tension generally can be related to pressure and phase composition and, quite often, decreases as the pressure and gas dissolution into the liquid phase each increase.[21]

Dimensionless Numbers in Characterizing Drop Stability. To characterize the stability of pendant drops used in the experiment, we examine dimensionless numbers. Many industrial processes involve the dispersion of immiscible fluids. The importance of interfacial tension can be illustrated using the dimensionless capillary number, *Ca*:

$$Ca = \frac{\eta\gamma R}{\sigma}$$

where η is the viscosity of the polymer, γ the applied shear rate, R the drop radius, and σ the interfacial tension between the immiscible phases.[32,33] The ratio of viscous force to surface force governs the situation between drop breakage and coalescence in many polymer blending and foaming processes. It determines the domain size of the polymer blends and the cell size of the polymer foams. For a small capillary number, the interfacial force dominates and a steady spherical drop shape exists. If the value is higher than a critical value, the drop is unstable and drop breakage occurs. Within the range of $0.1 < Ca < 10$, both coalescence and breakage phenomena take place simultaneously.[32] The *Ca* numbers of our pendant drop case must have been very small, and the system is in the interfacial force dominant range, because the shear rate was extremely small and the viscous force can be neglected.

The stability of the polymer pendant drop may be related to the Bond number, *Bo*:

$$Bo = \frac{\Delta\rho g R^2}{\sigma}$$

where $\Delta\rho$ is the density difference between two phases, g the gravitational acceleration, R the drop radius, and σ the interfacial

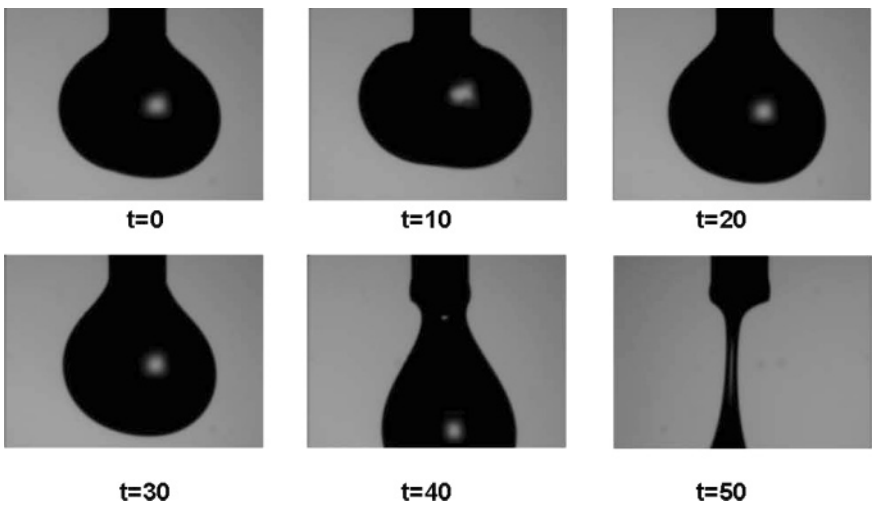

Figure 15. Evolution of polymer melts having a higher volume than a critical volume.

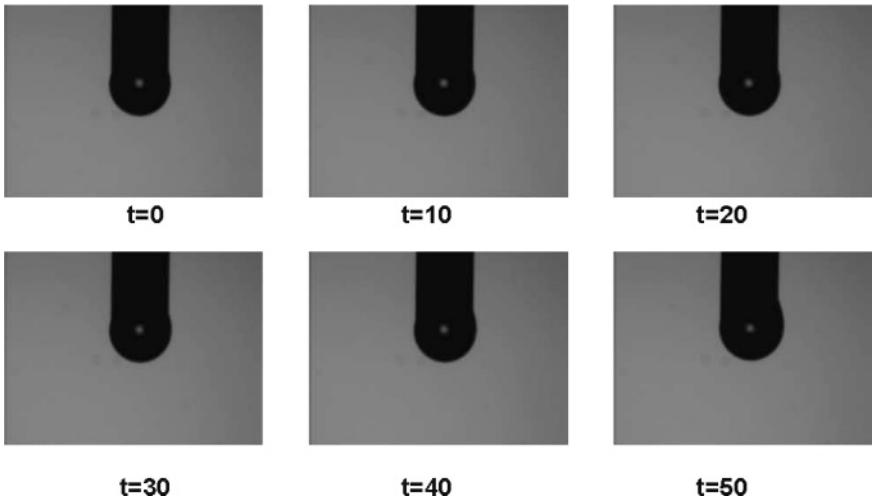

Figure 16. Evolution of polymer melts having a smaller volume than a critical volume.

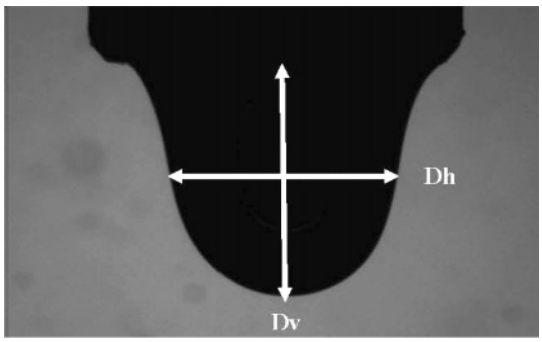

Figure 17. Graphical definition of the drop radius: drop radius = $[(D_v/2) + (D_h/2)]/2$, where D_v is the vertical diameter and D_h is the horizontal diameter.

tension between the immiscible phases.[2] The Bond number *Bo* is the ratio of buoyancy force to surface force. The number is used to indicate whether breakage occurs or the stable pendant drop is maintained. For a small Bond number *Bo*, the interfacial force is dominant and the drop shape is stable. If the number is higher than a critical value, the drop is unstable and drop breakage will occur. Other researchers have similarly verified these phenomena.[15,20]

In their pendant drop study, Ferri et al. demonstrated that the *Bo* values can be in the range of $Bo = 0.1-0.22$.[34] In our study, the drop size was optimized to achieve a stable pendant drop, and *Bo* was useful to determine whether the drop was stable. For large drop sizes, the pendant drops were unstable and breakage occurred, because of the dominant gravity force. When the drop was at a critical volume, the Bond number became $Bo = 1.4$, which is greater than 1, and the pendant drop detached from the feeding rod (see Figure 15). However, when the drop was smaller than a certain critical volume, the Bond number was $Bo = 0.2$, which is close to the lower limit of the critical value of 0.1,[34] and the drop liquid climbed up along the feeding rod (see Figure 16). In the present study, a Bond number in the range of $Bo = 0.4-0.8$ can avoid the drop breakage and liquid climb-up. The *Bo* range is higher than that of Ferri et al.,[34] which may be due to high viscosity of the polymer melt. Figure 17 shows how the vertical radius and the horizontal radius are defined to calculate the *Bo* value. The vertical diameter (D_v) is defined as the distance between the apex of the drop and the capillary tip, whereas the horizontal diameter (D_h) is defined as the horizontal distance at the center of the vertical diameter. The radius of the drop in *Bo* calculations was the average of the vertical radius and the horizontal radius.

Summary

The surface tension of polystyrene (PS) melts in supercritical CO_2 at temperatures of 210 and 230 °C was measured using the Axisymmetric Drop Shape Analysis-Profile (ADSA-P) method and was correlated with the solubility of CO_2 in PS. At higher pressures, the surface tension yielded lower values. After the critical pressure of carbon dioxide was achieved, the surface tension continued to decrease as the pressure increased. The empirical Macleod equation was applied to describe the relationship between the surface tension and the density differences of the two phases. The dimensionless parameters were used to characterize the stability of polymer pendant drops.

Literature Cited

(1) Myers D. *Surfaces, Interfaces, and Colloids: Principles and Applications*; VCH Publishers: New York, 1991.

(2) Adamson, A. W.; Gast, A. P. *Physical Chemistry of Surfaces*; Wiley: New York, 1997.

(3) Andreas, J. M.; Hauser, E. A.; Tucker, W. B. Boundary Tension by Pendant Drops. *J. Phys. Chem.* **1938**, *42*, 1001.

(4) Lahooti, S.; Rio, O. I.; Cheng, P.; Neumann, A. W. Axisymmetric Drop Shape Analysis (ADSA). In *Applied Surface Thermodynamics*; Neumann, A. W., Spelt, J. K., Eds.; Marcel Dekker: New York, 1996.

(5) Rotenberg, Y.; Boruvka, L.; Neumann, A. W. Determination of Surface Tension and Contact Angle from Shapes of Axisymmetric Fluid Interfaces. *J. Colloid Interface Sci.* **1983**, *93*, 169.

(6) Anastasiadis, S. H.; Chen, J. K.; Koberstein, J. T.; Siegel, A. F.; Sohn, J. E.; Emerson, J. A. The Determination of Interfacial Tension by Video Image Processing of Pendant Fluid Drops. *J. Colloid Interface Sci.* **1987**, *119*, 55.

(7) Miller, R.; Joos, P.; Fainerman, V. B. Dynamic Surface and Interfacial Tensions of Surfactant and Polymer Solutions. *Adv. Colloid Interface Sci.* **1994**, *49*, 249.

(8) Song, B.; Springer, J. Determination of Interfacial Tension from the Profile of a Pendant Drop Using Computer-Aided Image Processing. *J. Colloid Interface Sci.* **1996**, *184*, 77.

(9) del Rio, O. I.; Neumann, A. W. Axisymmetric Drop Shape Analysis: Computational Methods for the Measurement of Interfacial Properties from the Shape and Dimensions of Pendant and Sessile Drops. *J. Colloid Interface Sci.* **1997**, *196*, 136.

(10) Roe, R.-J.; Bacchetta, V. L.; Wong, P. M. G. Refinement of Pendant Drop Method for the Measurement of Surface Tension of Viscous Liquid. *J. Phys. Chem.* **1967**, *71*, 4190.

(11) Roe, R.-J. Surface Tension of Polymer Liquids. *J. Phys. Chem.* **1968**, *72*, 2013.

(12) Wu, S. Surface and Interfacial Tensions of Polymer Melts. II. Poly(methyl methacrylate), Poly(*n*-butyl methacrylate), and Polystyrene. *J. Phys. Chem.* **1970**, *74*, 632.

(13) Wu, S. *Polymer Interface and Adhesion*; Marcel Dekker: New York, 1982.

(14) Anastasiadis, S. H.; Chen, J. K.; Koberstein, J. T.; Sohn, J. E.; Emerson, A. The Determination of Polymer Interfacial Tension by Drop Image Processing: Comparison of Theory and Experiment for the Pair, Poly(dimethyl siloxane)/Polybutadiene. *Polym. Eng. Sci.* **1986**, *26*, 1410.

(15) Demarquette, N. R.; Kamal, M. R. Interfacial Tension in Polymer Melts. I: An Improved Pendant Drop Apparatus. *Polym. Eng. Sci.* **1994**, *34*, 1823.

(16) Kwok, D. Y.; Cheung, L. K.; Park, C. B.; Neumann A. W. Study on the Surface Tensions of Polymer Melts Using Axisymmetric Drop Shape Analysis. *Polym. Eng. Sci.* **1998**, *38*, 757.

(17) Wulf, M.; Michel, S.; Grundke, K.; del Rio, O. I.; Kwok, D. Y.; Neumann, A. W. Simultaneous Determination of Surface Tension and Density of Polymer Melts Using Axisymmetric Drop Shape Analysis. *J. Colloid Interface Sci.* **1999**, *210*, 171.

(18) Funke, Z.; Schwinger, C.; Adhikari, R.; Kressler, J. Surface Tension in Polymer Blends of Isotactic Poly(propylene) and Atactic Polystyrene. *Macromol. Mater. Eng.* **2001**, *286*, 744.

(19) Morita, A. T.; Carastan, D. J.; Demarquette, N. R. Influence of drop volume on surface tension evaluated using the pendant drop method. *Colloid Polym. Sci.* **2002**, *280*, 857.

(20) Xue, A.; Tzoganakis, C.; Chen, P. Measurement of Interfacial Tension in PS/LDPE Melts Saturated With Supercritical CO_2. *Polym. Eng. Sci.* **2004**, *44*, 18.

(21) Li, H.; Lee, L. J.; Tomasko, D. L. Effect of Carbon Dioxide on the Interfacial Tension of Polymer Melts. *Ind. Eng. Chem. Res*. **2004**, *43*, 409.

(22) Bashforth, F.; Adams, J. C. *An Attempt to Test the Theories of Capillary Action*; University Press: Cambridge, England, 1883.

(23) Sanchez, I. C.; Lacombe, R. H. An Elementary Molecular Theory of Classical Fluids. Pure Fluids. *J. Phys. Chem.* **1976**, *80*, 2352.

(24) Sato, Y.; Takikawa, T.; Takishima, S.; Masuoka, H. Solubilities and diffusion coefficients of carbon dioxide in poly(vinyl acetate) and polystyrene. *J. Supercrit. Fluids* **2002**, *19*, 187.

(25) Li, G.; Wang, J.; Park, C. B.; Moulinie, P.; Shimha, R. *Annu. Tech. Conf.—Soc. Plast. Eng.* **2004**, Paper No. 421.

(26) *CRC Handbook of Chemistry and Physics*; CRC Press: Cleveland, OH, 1981.

(27) Milton, J. S.; Arnold, J. C. *Introduction to Probability and Statistics*; McGraw−Hill: New York, 1995.

(28) Gonzalez, G.; MacRitchie, F. Equilibrium Adsorption of Proteins. *J. Colloid Interface Sci.* **1970**, *32*, 55.

(29) Miller, R.; Kretzschmar, G. Adsorption Kinetics of Surfactants at Fluid Interfaces. *Adv. Colloid Interface Sci.* **1991**, *37*, 97.

(30) Macleod, D. B. On a Relation between Surface Tension and Density. *Trans. Faraday Soc.* **1923**, *19*, 38.

(31) Ferguson, A.; Kennedy, S. J. Free and Total Surface Energies and Related Quantities. *Trans. Faraday Soc.* **1936**, *32*, 1474.

(32) Tomasko, D. L.; Li, H.; Liu D.; Han, X.; Wingert, M. J.; Lee, L. J.; Koelling K. A Review of CO_2 Applications in the Processing of Polymers. *Ind. Eng. Chem. Res.* **2003**, *42*, 6231.

(33) Janssen, J. M. H.; Meijer, H. E. H. Droplet breakup mechanisms: Stepwise equilibrium versus transient dispersion. *J. Rheol. (N.Y.)* **1993**, *37* (4), 597.

(34) Ferri, J. K.; Lin, S. Y.; Stebe, K. J. Curvature Effects in the Analysis of Pendant Bubble Data: Comparison of Numerical Solutions, Asymptotic Arguments and Data. *J. Colloid Interface Sci.* **2001**, *241*, 154.

Received for review August 4, 2005
Revised manuscript received November 28, 2005
Accepted January 4, 2006

IE0509084